Chapter 9

Synthesis of Graphene on Metal/SiC Structure

Petr Machac

Additional information is available at the end of the chapter

http://dx.doi.org/10.5772/67465

Abstract

The chapter deals with the synthesis of graphene on metal/SiC substrates. The graphene synthesis is pursued at a relatively low temperature. The method can be used for the graphene transfer from SiC to dielectric materials. Annealing of the structure results in a chemical reaction of a metal with SiC forming silicides and carbon-rich products at the boundary between metal and silicon carbide. Carbon atoms segregate at the top of metal/metal silicide layer during the cooling period of the process. The chapter is divided into the following sections: Introduction, Structure preparation, Graphene preparation from the structure Ni/SiC, Graphene preparation from the structure Co/SiC, Application of other metals, Influence of additive materials, and Conclusion.

Keywords: graphene, nickel, cobalt, Raman spectroscopy, graphene transfer

1. Introduction

Graphene is a 2D form of graphite which can be used in electronics and other branches of technique due to its interesting parameters [1–3]: high electron mobility—in literature, the published value was at 1.5×10^8 m^2/Vs, very low resistivity (1×10^{-4} Ωm), metallic and semiconductive character, low absorption of white light (2.3%), low noise, quantum Hall effect, and so on. These important parameters predestine graphene for substitution of silicon in future microelectronics. Application of graphene is expected for construction of field effect transistor (FET) transistors, transparent conductive electrodes, gas and biosensors, lithium batteries, memory structures, super capacitors, and other structures [2]. The so-called single-layer graphene (SLG) shows the widest application; so the preparation of few layer graphenes (FLG) can be usually simpler.

Graphene is grown by many technological processes. The method of mechanical exfoliation or cleavage was one of the first methods, used by Geim and Novoselov, for the preparation of the graphene films [4–6]. This method comes from mechanical splitting of thin pieces of

graphite from the oriented pyrolytic graphite. The main disadvantage of the method is that it produces only small pieces of graphene—graphene flakes.

Today, many methods are used for graphene growth. Graphene is very frequently prepared by a chemical vapor deposition (CVD) method [7–9]. Thin foils of Cu, Ni, or other metals are used as substrates. The method is scalable (graphene films with large dimension can be prepared), but the graphene film must be transferred onto a dielectric substrate for the next application (e.g., SiO_2/Si). Temperature or plasma CVD processes are used in practice.

The next method is a high-temperature decomposition of SiC, which is sometimes called as an epitaxial growth of graphene (EG) [10–12]. In the method silicone atoms sublimate from the surface of SiC substrate at high temperature—1100–1600°C in high vacuum and remaining carbon creates graphene. The method can be used for industrial growth of graphene due to full-wafer technology. Careful control of the sublimation process has recently led to the growth of very thin graphene film over the SiC surface, with only single graphene layer.

The vacuum sublimation of SiC usually produces graphene films with small crystallinity (30–200 nm) [13, 14] due to surface SiC roughening and creation of deep pits. The preparation of graphene by decomposition of SiC in an argon atmosphere of about 100 kPa gives better layers. This method gives SLG films with greater domain sizes. Graphene parameters can be also improved by increasing the growth temperature (up to 2000°C) since SiC decomposition occurs at 1500°C under argon atmosphere rather than at 1150°C in vacuum.

A special sort of method of graphene preparation is the so-called transfer-free method [15]. The method comes from a metal/C/SiO_2/Si structure. The synthesis of graphene is based on a metal-catalyzed crystallization of amorphous carbon (a-C) by thermal annealing. Polymer layer [16] and thin SiC layer [17] are used very frequently as the carbon source instead of a-C. Carbon atoms diffuse into a metal layer at elevated temperatures followed by their precipitation as graphene during the cool-down step.

The graphene growth on SiC substrates at relatively low temperature is very perspective [18]. The technique applies the Ni/SiC system as a basic structure. The method is very promising for the transfer of graphene layers from the SiC substrate to other substrates (mainly on dielectric one). By the annealing of the Ni/SiC system, carbon-rich products can be obtained at the Ni-SiC interface, and the graphene film is segregate on the top of the Ni layer.

This method has been developed by various groups of authors in many ways. The Ni(200 nm)/SiC structure was applied in the work [18]. Graphene was grown on the structure surface by annealing at 750°C (the speed of 25°C per second), with follow-up cooling with no specified velocity. The prepared graphene showed the FLG character. The results of the mentioned work are in discrepancy with the results of works [19, 20], where only thin Ni films (from single to tens nm) were applied. Heating speed was slightly lower (4°C per second), and cooling velocity was approximately 20°C per second. Prepared graphene had a character of FLG and SLG. Authors of work [21] elaborated with the Ni/SiC structure, where the thickness of nickel layer did not exceed the value of 100 nm. The annealing of the structure produced at 1100°C for 300 s (heating and cooling velocities were not specified; a rapid thermal process was used). After the annealing process, the created silicide layer was etched off, and a thin graphene film of FLG type remained on the silicon carbide substrate. Lastly, the modificated method described in the study [22] is also valuable. A

http://dx.doi.org/10.5772/67465

50 nm-thick amorphous silicon carbide layer was used here. The layer was deposited onto the SiO_2/Si substrate, and after that, the SiC layer was covered with 500 nm of Ni. Annealing was done by an Rapid Thermal Annealing (RTA) process at 1100°C for 30 s. The formed silicide was etched off, and the graphene film was detected on the SiO_2 surface. Co as a metal can be used too instead of Ni [23]. The segregation method can be applied in case of metal combination for reduction of carbon solubility and thus modification of the segregation process itself. Ni/Cu metallization was used in Ref. [24] for the preparation of graphene films in silicon carbide-based Micro Electro Mechanical Systems (MEMS) and Nano Electro Mechanical Systems (NEMS) devices.

2. Structure preparation

N-type 4H-SiC substrate wafers, Si-face polished, 4° off-axis, and doping level 4×10^{18} cm^{-3} (supplied by SiCrystal A.G.) were used in our experiments. Majority of metallization were deposited using e-beam evaporator at 135°C in the vacuum of 2×10^{-4} Pa; alternatively, a DC magnetron sputtering apparatus with Ar plasma was used. Prior to the deposition of metals, the wafers were cleaned by the following wet chemical process: 5 min in acetone (ultrasound bath), 5 min in $NH_4OH:H_2O:H_2O_2$ (5:1:1) (ultrasound bath), 5 min in 5% HF (ultrasound bath), 10 min in boiling water, and finally drying by nitrogen.

Graphene films were produced by thermal treatment of metal/SiC structures in a small vacuum chamber equipped with a resistively heated table (Boralectric heating element). First off, samples were degassed at 300°C for 5 min and then annealed at 600–1100°C in a pressure bellow 3×10^{-4} Pa. Temperature was measured with an optical pyrometer. Heating rate was approximately 17.5°C/s and cooling rate was 15°C/s.

Samples were analyzed by means of the Raman spectroscopy using a DXR Raman microscope spectrometer of the company Thermo Fisher Scientific equipped with confocal Olympus microscope. Solid-state Nd:YAG laser (wavelength 532 nm, maximum power 10 mW) was used as excitation source. Measurement conditions were 7 mW power, ten accumulations of 10 s. scans, grating with 900 lines/mm, and aperture 50 μm slit. A multichannel thermoelectrically cooled Charge Coupled Device (CCD) camera was used as detector. Magnification 50x provided measurement spot size ~1 μm^2. For X-ray photoelectron spectroscopy (XPS), measurements were applied in two apparatus. Majority of the measurement were done in an ESCAProbe P apparatus from Omicron NanoTechnology Ltd. (vacuum 10^{-8} Pa, Al anode, energy of monochromated X-ray source 1486.7 eV, analyzed area with size of 1 mm^2, depth profiling by Ar ions sputtering). Alternatively, for XPS measurement was apply a NanoESCA apparatus from Omicron NanoTechnology Ltd. equipped with a photoemission electron microscopy navigation technique. The apparatus obtained these radiation sources: Hg-lamp (5.2 eV), HeI (21.2 eV), and a monochromatic X-ray source Al K-alpha (1486.7 eV). The spectra processing and evaluation were produced by CasXPS software. Peak component fitting was done by symmetric Gaussian (70%)-Lorentzian (30%) peaks and Shirley background. Atomic force microscopy (AFM) analysis was conducted in a Veeco CP II apparatus in the tapping mode. Photos on structures were made on an optical microscope Jenavert G0685, magnification 2000. Electrical measurements were done on a computer-controlled workplace by a standard van der Pauw method.

3. Graphene preparation from the structure Ni/SiC

Growth of graphene films was done on a set of Ni/SiC structures with the different thickness of nickel layers (1, 5, 10, 50, 200, and 300 nm) and in the different type of thermal forming [25, 26]. Raman spectra were measured for all samples after annealing. The structure with the thinnest nickel layer showed the Raman spectrum with a very small G band, while the D and 2D bands were absent. Apparently, due to a shortage of Ni in this sample, the necessary quantity of carbon atoms for growth of graphene films by SiC decomposition was not released. So, this structure was omitted in the other text.

3.1. Raman spectroscopy

In **Figure 1**, an example of Raman spectra of structures differing in the thickness of the deposited nickel layer is shown. Annealing was carried out in the same way for all samples (heating temperature 1080°C, annealing period 10 s). All Raman spectra in **Figure 1** contain the main characteristic bands of carbon materials designated as D (1350 cm^{-1}), G (1580 cm^{-1}), and 2D (2700 cm^{-1}). The integral intensity ratio of the D and G bands (I_D/I_G) can be applied for the quantification of defects in graphene. An equation for the calculation of the crystallite size L_a in the graphene layer using any laser radiation can be written as [27]

$$L_a(nm) = \frac{560}{E^4(eV)}\left(\frac{I_D}{I_G}\right)^{-1} \quad (1)$$

where E is the energy of laser which was applied in the Raman analysis. The integral intensity ratio of the 2D and G bands (I_{2D}/I_G) can be applied for the calculation of carbon layer number in the graphene layer. Alternatively, the value of the 2D band full width at half maximum (FWHM) can be used [28]. SLG shows the value of I_{2D}/I_G in the range 3–3.5 (ideally 4), and FWHM of the 2D band is then 25 cm^{-1}.

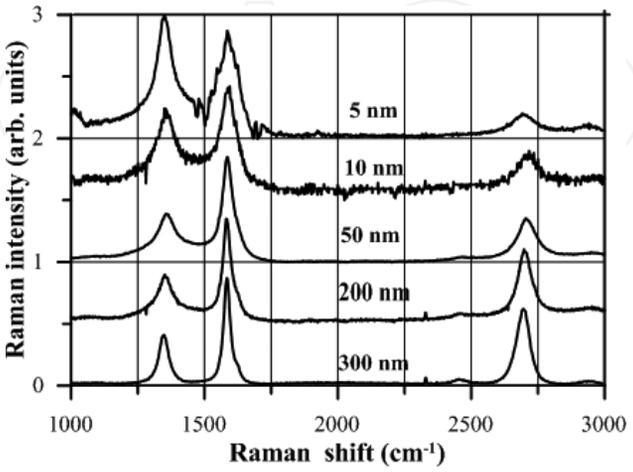

Figure 1. Raman spectra of Ni/SiC samples with Ni thickness in the range of 5, 10, 50, 200, and 300 nm. (Reprinted with permission from Thin Solid Films No. 3995281012757.).

http://dx.doi.org/10.5772/67465

It is obvious that the ratio I_{2D}/I_G from the Raman spectra of all samples on **Figure 1** increases, and opposite to the fact, the ratio I_D/I_G decreases, while the thickness of Ni layer is growing. The resulting graphene film then has less defects or bigger crystals, respectively, and contains smaller number of carbon monolayers for samples with a thicker Ni layer. The graphene film on the Ni(200)/SiC structure shows $I_D/I_G = 0.41$, $I_{2D}/I_G = 0.66$ and FWHM = 59 cm^{-1}. Using the data from Ref. [28] and the formula (1), the number of carbon monolayers was determined to be 3.8 and crystallite size L_a = 45 nm. The graphene film prepared on the Ni(300)/SiC structure is similar—the number of carbon monolayers is slightly lower (3.5), and crystallite size is lower too (40 nm).

Further, an influence of temperature of the annealing process on parameters of the graphene films was tested. **Figure 2** illustrates dependence of the I_{2D}/I_G ratio on the annealing temperature, which was gained from Raman spectra of the graphene films on the Ni(200 nm)/SiC structures. The films were prepared by annealing of the structure in the temperature changing from 710 to 1080°C. The annealing time was in all cases 10 s. From the obtained dependence, it is evident that the graphene film with minimal number of carbon monolayers was obtained in the case of the highest annealing temperature (1080°C).

We studied also the quality of carbon films that were formed at the boundary between the metallization and silicon carbide substrate (lower graphene). In these experiments the annealed metallization was etched off firstly. The etching was produced in the mixture of acids HNO_3:HF = 3:1 for 10 min. Analysis of the structures was carried out by the Raman measurement again. **Table 1** obtains the results—the values of ratios I_{2D}/I_G and I_D/I_G of the structures before (Ni surface) and after (SiC surface) the etching. It is evident from the results that the lower graphene film analyzed on the SiC surface showed for the most experiments higher I_{2D}/I_G ratio than in the graphene film on the metallization surface. Evidently, the graphene films on the SiC surface show a lower number of carbon monolayers. The great disadvantage of lower graphene is the much higher I_D/I_G ratio and so higher concentration of defects (smaller crystals). The crystallite size for the graphene film from the last line of **Table 1** is 67 nm before the etching and 16 nm after the etching of the nickel metallization.

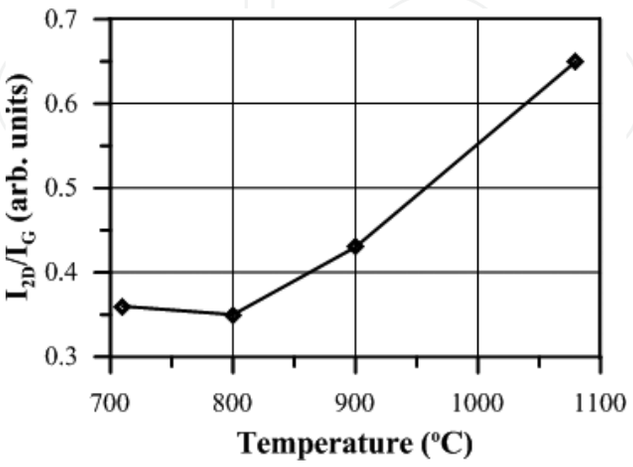

Figure 2. Ratio of 2D and G band intensities in Raman spectra of graphene on the Ni(200)/SiC structures annealed at various temperatures. (Reprinted with permission from Thin Solid Films No. 3995281012757.).

Parameters of graphene growth			Ni surface		SiC surface	
Thickness of Ni layer [nm]	**Annealing temperature [°C]**	**Annealing time [s]**	**I_D/I_G**	**I_{2D}/I_G**	**I_D/I_G**	**I_{2D}/I_G**
200	1080	10	0.40	0.65	1.20	0.46
200	1080	60	0.43	0.55	1.24	0.65
200	1080	180	0.27	0.50	1.10	0.67

Reprinted with permission from Thin Solid Films No. 3995281012757.

Table 1. Results of Raman analysis of the graphene structures (the ratios of band intensities) on the nickel surface and after the metallization was etched off (graphene on the SiC surface).

3.2. Thickness of graphene layers

The thickness of graphene films was calculated mainly from a dependency between the number of carbon monolayers and the I_{2D}/I_G ratio along with the FWHM obtained from Raman spectra [28]. An example is shown in **Table 2**. It shows values of the number of carbon monolayers (N) that were determined concurrently from the I_{2D}/I_G ratio and from the FWHM. There is a quite good conformity among the values. The values of N determined from the I_{2D}/I_G ratio are a bit higher than the values determined from the FWHM.

The XPS analysis was used for verification of the results in the case of the Ni(200 nm)/SiC structure (annealing temperature 1080°C, annealing time 10 s). The process is based on the attenuation of photoelectrons that are excited from the material under the graphene film [3]. Thickness of the graphene film can be determined from the formula

$$d = -\lambda \ln(I/I_o), \tag{2}$$

where I and I_o are intensities of XPS signal of a selected element that was measured on the surface of the graphene film and from the material under the graphene film, respectively. λ represents inelastic mean free path of electrons in the graphene film. Signal of Ni_2 p3/2 with the electron energy of 853 eV was selected in our experiments. The value of $\lambda = 2.4$ nm was gained from literature [29]. The surface of the graphene film was analyzed at first (I = 400 electron/s), and then the film was progressively sputtered off with Ar ions. Intensity of the Ni_2 p3/2 signal $I_o = 4500$ electron/s was reached when the graphene film was completely removed. Thickness

Parameters of graphene growth			I_{2D}/I_G	N	FWHM	N
Thickness of Ni [nm]	**Annealing temperature [°C]**	**Annealing time [s]**				
200	1080	0	0.53	5	66	4.7
200	1080	10	0.65	3.8	59	3.4

Reprinted with permission from Thin Solid Films No. 3995281012757.

Table 2. Number of carbon monolayers N for the chosen graphene structures.

http://dx.doi.org/10.5772/67465

of the graphene film 2.5 nm was calculated from the formula (2). The number of carbon monolayers in the prepared graphene film can be gained by dividing the obtained thickness of graphene film by the thickness of the monolayer of carbon (0.335 nm). In graphene films, however, the distance of carbon monolayers can change from 0.55 to 0.70 nm [30]. So we can conclude that the number of carbon monolayers in the graphene film on the Ni(200 nm)/SiC structure shows value from 3.6 to 4.5 and it corresponds to the data in **Table 2**.

3.3. Graphene morphology

The morphology of structure surfaces was studied by the AFM measurement. **Figure 3** shows the surface morphology of the Ni(300 nm)/SiC structure annealed at 1000°C for 120 s. Massive reaction of the nickel film with SiC substrate occurred in the annealing process, and the reaction was not homogeneous which is confirmed by large roughness R_a = 31 nm. The prepared graphene film lays on the metallization surface, and consequently it shows large number of defects and thus has low crystallinity.

3.4. Graphene transfer

Figure 4 shows an example of Raman spectra of a structure after annealing at 950°C, annealing period 30 s. The solid line represents spectrum after the annealing; the dashed line represents spectrum of the graphene film transferred onto the SiO_2/Si substrate. The transfer was done by the etching of the silicide layer by the mixture of HF and HNO_3 acids (ratio 3:1) and with help of polymethyl methacrylate (PMMA). It is possible to estimate that graphene from **Figure 4** contains four carbon layers, its crystallite size is 43 nm, and the transfer increases its value on 82 nm. The difference is probably done by smoother surface of SiO_2.

3.5. Electrical parameters

The basic electronic parameters of prepared graphene were measured. Experiments were done with the metallization prepared by the evaporation of nickel (thickness of 300 nm). For the measurements it is necessary to have a dielectric substrate; therefore, a semi-insulating SiC plate

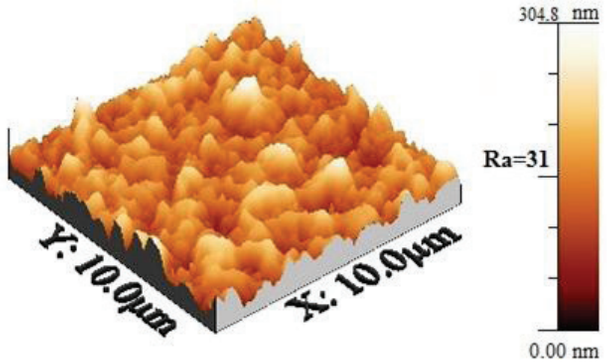

Figure 3. AFM picture of the graphene film surface prepared on the Ni(300)/SiC structure annealed at 1000°C for 120 s. (Reprinted with permission from J Electrical Engineering.).

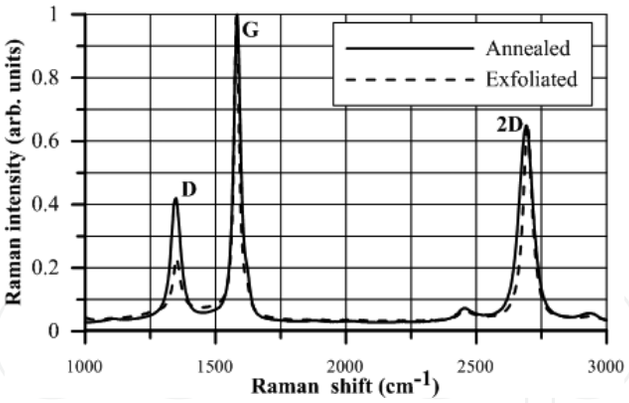

Figure 4. Raman spectra of Ni/SiC sample after the annealing and after the exfoliation. (Reprinted with permission from J Electrical Engineering.).

(SI-SiC) was used, and the graphene film on the interface between SiC and the metallization was tested (after the annealing, the silicide layer was etched off by HNO_3 acid, and the graphene/SI-SiC structure was obtained). For the measuring of electrical parameters by van der Pauw method, the Au(30)/Cr(10) contacts prepared by evaporation were applied. Obtained results are shown in **Table 3** (ρ_s is surface resistivity, μ_H is Hall mobility, and c_s is the concentration of charge carriers). Hall mobility of the prepared graphene films is very low probably due to large concentration of defects in graphene layers.

3.6. Conclusion

The synthesis of graphene on silicon carbide substrates by the Ni-silicidation reaction shows two significant advantages:

- It needs a relatively low temperature for graphene growth (up to 1100°C) compared to the preparation of epitaxial graphene on SiC (minimally 1300°C).
- It needs short process time (from several seconds to several minutes) compared to the CVD method (from several minutes to several hours).

The method is scalable—so it can be applied for the growth of large-area graphene films. However, the technique has a disadvantage—the graphene films are prepared on the conductive plate. For application in microelectronics (unipolar transistors and other devices), the transfer on the dielectric substrate (SiO_2/Si) is necessary. Alternatively, it is possible to apply

Annealing conditions		ρ_s (Ω)	μ_H (cm²/Vs)	c_s (cm⁻²)
T (°C)	t (s)			
1050	60	527 ± 2.5	300 ± 7.3	$3.85 \times 10^{13} \pm 7.3 \times 10^{11}$

Reprinted with permission from J Electrical Engineering.

Table 3. Electrical parameters of graphene on SI SiC.

semi-insulating SiC substrate together with the lower graphene. The formed silicide layer must be etched off. The lower graphene film can be applied directly for the preparation of electronic devices.

The following conclusion can be done from the results. In our experiments, the Ni films of assorted thicknesses ranging from 1 to 300 nm were applied. Graphene was grown on all samples except one with Ni 1 nm thick. The Ni(200 nm)/SiC structure produced the best results. The quality of lower graphene films growth on the SiC surface was studied after removing of the annealed metallization. In majority of cases, lower graphene films were thinner, but they showed lower crystallinity, which was caused by rough SiC surface after the reaction of Ni with silicon carbide. Thermal forming of the Ni/SiC structures was carried out at the temperature range from 710 to 1080°C and for diverse times. The temperature of 1080°C and time of 10 s showed the best process conditions. The graphene film with character of FLG (the number of carbon monolayers in the range from 3 to 4) was produced on the base of the Ni(200 nm)/SiC structure. Longer annealing period had no noticeable influence to the graphene film parameters. Thickness of the graphene films was checked up by the XPS analysis; the value of 2.5 nm was obtained for the mentioned sample, which is similar to the value gained from the results of Raman spectroscopy. Very good agreement in results was given by both independent methods.

4. Graphene preparation from the structure Co/SiC

Graphene films were prepared by thermal processing of the Co/SiC structures, which differed in thickness of the cobalt layer (10, 50, 100, 200, and 300 nm) [31–33]. Co deposition was performed using a DC magnetron sputtering apparatus at room temperature. Alternatively, the Co layer with thickness 300 nm was deposited by the e-gun evaporation. For studying basic parameters of the prepared graphene films, Raman spectroscopy was chosen.

4.1. Raman spectroscopy

Raman spectra of several Co/SiC structures, which differ in thickness of the Co layer [31], are shown on **Figure 5**. The spectra were normalized to the same size of the G band, in order to compare D and 2D bands. All structures were formed at temperature of 1080°C, and the annealing period was 10 s. The graphene film was not prepared for the structure with 10 nm-thick cobalt layer. The resulting layer shows character of amorphous carbon with very low thickness (the signal is very weak—especially, the 2D band and the spectrum are noisy). With increasing thickness of the Co layer, the 2D band intensity grows up. This gives evidence of decreasing number of carbon monolayers in the formed graphene film. There is about five carbon monolayers for the structure Co(50 nm)/SiC. In the case of the structure with the thickest cobalt layer, a three-layered graphene film has been created. Similarly, crystallinity of the formed graphene films improves when thickness of the Co layer is growing. In the case of the structure Co(300 nm)/SiC, the crystal size in the graphene film is approximately 110 nm.

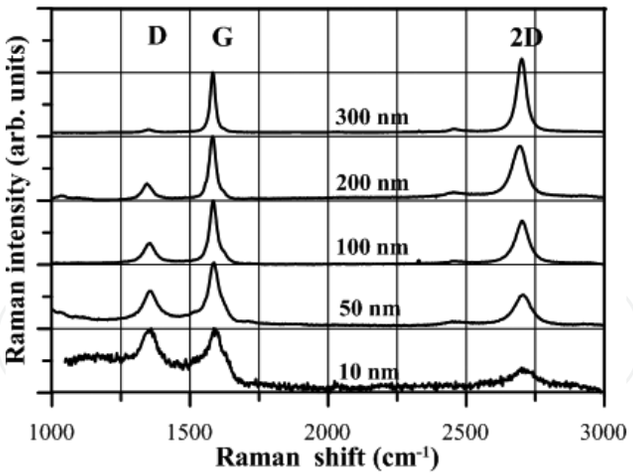

Figure 5. Raman spectra of several Co/SiC structures differing in Co layer thickness. (Reprinted with permission from J Mater Sci: Mater Electron, No. 3995250684677.).

An interesting effect was noticed at the structure Co(300 nm)/SiC. In the case of shorter annealing periods and in dependence on the graphene growth temperature, two different phases have emerged on the surface of the structures—a dark and a light. With the increasing of annealing period, the area of the dark-phase domain was increasing, and, finally, it was spreading over the whole area of the structure. Quality of the structure surface was nevertheless worse. **Figure 6** shows a photograph of the structure Co(300 nm)/SiC annealed at 990°C for 60 s. From the analysis in **Figure 7**, it is obvious that the dark phase contains the graphene film and cobalt silicides, while the light one does not include graphene and silicides. The XPS analysis has been used for verification of the phenomena [31]. The reaction of Co with SiC starts probably at defects and then gradually propagates over the surface of the structure. The effect does not occur at structures with a thinner cobalt layer, and their surface is smoother and homogenous [31].

Figure 6. Example of a structure surface with Co layer 300 nm thick annealed at 990°C for 60 s. (Reprinted with permission from J Mater Sci: Mater Electron, No. 3995250684677.).

http://dx.doi.org/10.5772/67465

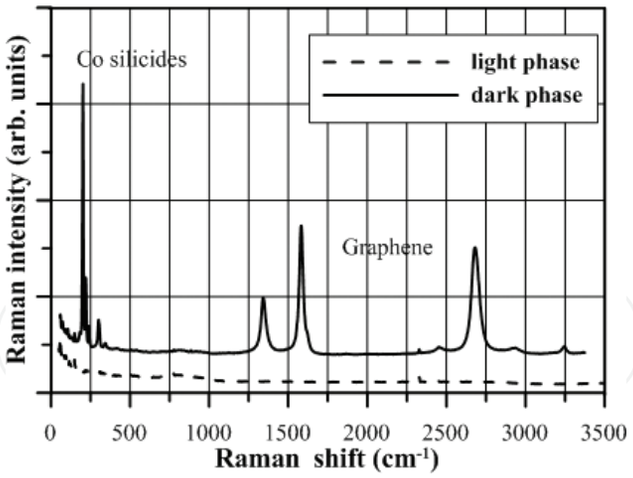

Figure 7. Raman spectra of the Co(300 nm)/SiC structure annealed at 990°C for 60 s. (Reprinted with permission from J Mater Sci: Mater Electron, No. 3995250684677.).

Slightly, other results were obtained in the case of cobalt layers prepared by evaporation [32]. The metallization was deposited onto SiC substrates at elevated temperature (135°C). The substrates were treated in situ by DC Ar plasma before the metal deposition. The layer thickness was 300 nm (the best thickness from previous research) [31]. **Figure 8** shows dependence of the I_{2D}/I_G ratio on annealing time of the structure annealed at 850°C. The results confirm that the sample annealed for 10 s is the best and shows character of nearly BLG. Contrary to the earlier work [31], there has not been observed formation of two phases on the sample surface during graphene growth. Samples' surface was homogenous after annealing, and the graphene phase spread all over the surface.

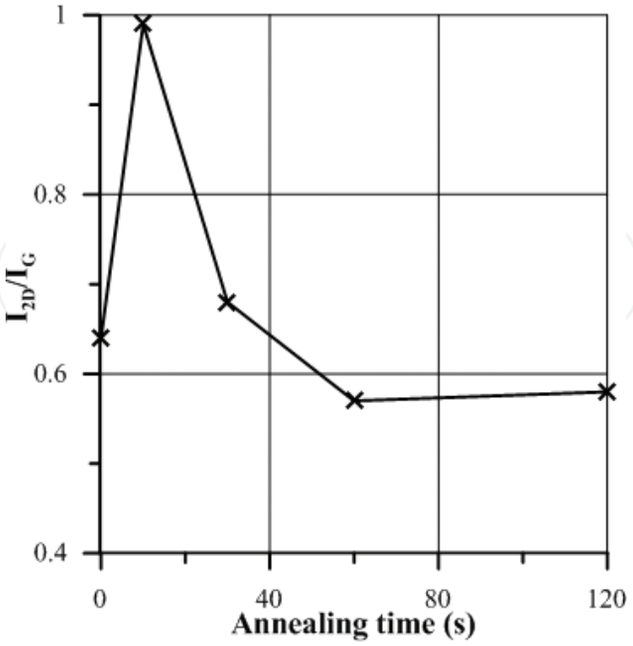

Figure 8. Ratio of 2D and G band intensities in Raman spectra of graphene prepared by annealing at 850°C and at various times. (Reprinted with permission from Applied Surface Science No. 3995260811830.).

4.2. Graphene exfoliation

Graphene films grown on the structure metal/SiC are not suitable for direct application in microelectronics. This is because of graphene having been produced by the reaction of a metal with silicon carbide leading to formation of silicides and carbon. The graphene film is created on a layer of silicides with large electrical conductivity, and thus it does not allow constructing electronic structures (such as unipolar transistor). A certain opportunity is to apply the lower graphene film which is created at the SiC-metal boundary. This graphene film shows however worse parameters than the surface graphene film (the graphene film on the silicide layer) [25]. Preparation of the lower graphene was tested with the Co/SiC structure as well [31]. **Table 4** shows results, which, apart from basic parameters of the technological process, contain also the values of I_{2D}/I_G and I_D/I_G before etching (the surface graphene) and after etching (the lower graphene on the surface of SiC substrate). It is evident from the table that the lower graphene shows in majority cases worse values of the I_{2D}/I_G and I_D/I_G ratios.

Another possibility to form a graphene film on a nonconductive substrate is to transfer the graphene film from the Co/SiC structure onto a dielectric substrate (SiO_2/Si). **Table 4** shows an example of obtained results—the last two columns in the table. It is evident from the table that the transfer of graphene has smaller influence on its parameters than the preparation of the lower graphene. In addition, the silicon carbide surface after the etching-off of the metallic layer evinces greater surface roughness than with the transferred graphene.

Graphene films prepared on the metal/SiC structure are not appropriate for direct measurements of electrical parameters since they are situated on a conductive silicide layer. So it is necessary to transfer the graphene film on a dielectric substrate. **Table 5** gives the example of an obtained result [32]. The table includes parameters (sheet resistance, mobility, and hole concentration) of the graphene film prepared by the annealing of the Co(300 nm)/SiC structure at 1050°C for 120 s. The graphene film has been transferred onto the SiO_2/Si substrate.

4.3. Influence of cooling rate

Authors of a number of studies, which deal with growing of graphene by synthesis on metal/SiC structures [18, 20, 23, 34], postulated that parameters of graphene films are dependent on the cooling rate (CR) of the structures after the annealing is stopped. We have tried to verify the statement experimentally. The structures annealed at 1050°C for 120 s were chosen for

Technological parameters			Surface graphene		Lower graphene		Exfoliated graphene	
Co layer thickness [nm]	Annealing temperature [°C]	Annealing time [s]	I_{2D}/I_G	I_D/I_G	I_{2D}/I_G	I_D/I_G	I_{2D}/I_G	I_D/I_G
300	1080	120	0.76	0.34	0.75	0.66	0.63	0.06
100	1080	120	0.76	0.10	0.88	0.37	0.73	0.20

Table 4. Basic parameters of graphene films—surface graphene, lower graphene, and exfoliated graphene.

Sheet resistance [Ω]	Mobility [cm²/Vs]	Hole concentration [cm⁻²]
529	433	2.73×10^{13}

Table 5. Electrical parameters of the graphene layer after the exfoliation process.

the experiment. The tested structures were mounted on a special molybdenum tray prior to the annealing process, and the tray was resistively heated by large current. The tray enables us to control cooling temperature within the CR from 2 to 70°C/s. The highest CR is given by switching off a power supply, and the structure cools down independently. The CR was set by controlling the passing current. **Figure 9** shows the results. The graph represents dependence of the resulting I_{2D}/I_G and I_D/I_G ratios of prepared structures on the CR. It is obvious from the graph that the CR has nearly no influence onto the I_{2D}/I_G ratio (the number of carbon monolayers in the graphene film). However, the CR has a significant influence on the I_D/I_G ratio (the number of defects in the prepared graphene film). The faster cooling is the more defects in the graphene films are created.

4.4. XPS analysis

The analysis was performed on the structure Co(300 nm)/SiC which was prepared by the evaporation process [32]. The structure for the XPS analysis is special, unlike regular structures. The cleaning, annealing, and analyzing of the sample were done in the NanoESCA apparatus. The sample was inserted into the apparatus, and the process of the experiment was done as follows:

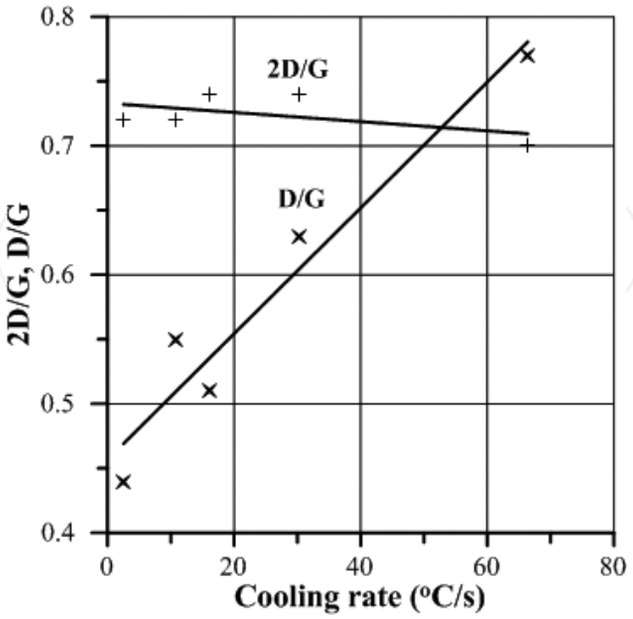

Figure 9. I_{2D}/I_G and I_D/I_G ratios for different cooling rates. (Reprinted with permission from Thin Solid Films No. 3995281012757.).

- Degassing at 250°C for 12 h.
- Cleaning by a 1 keV Ar sputtering at 2×10^{-4} Pa for 20 min.
- Annealing at 850°C for 10 s.

A vacuum of 5×10^{-9} Pa was kept in the apparatus chamber during the process.

XPS analysis was performed in the sample's as-received state, after the sputtering and finally after the annealing. **Figure 10** shows all three survey spectra. The spectrum of as-received sample surface includes oxygen, carbon, and cobalt. Co and O probably create a native cobalt surface oxide, and carbon probably comes from an atmospheric contamination [35–37]. The sample surface after the sputtering is evidently free from C, and presumably the oxygen concentration likewise decreased. Silicon peaks appeared, and O is desirably absent at the sample after the annealing. The appeared Si is a product of the reaction between Co and SiC which yields Co silicides and free C [38, 39]. So Co and C are detected simultaneously. **Table 6** summarizes the atomic concentrations of all elements.

Detail spectra, which contain only narrow scans, are presented in the next paragraphs and figures with aim to give us a deeper chemical investigation. Firstly, it should be pointed out

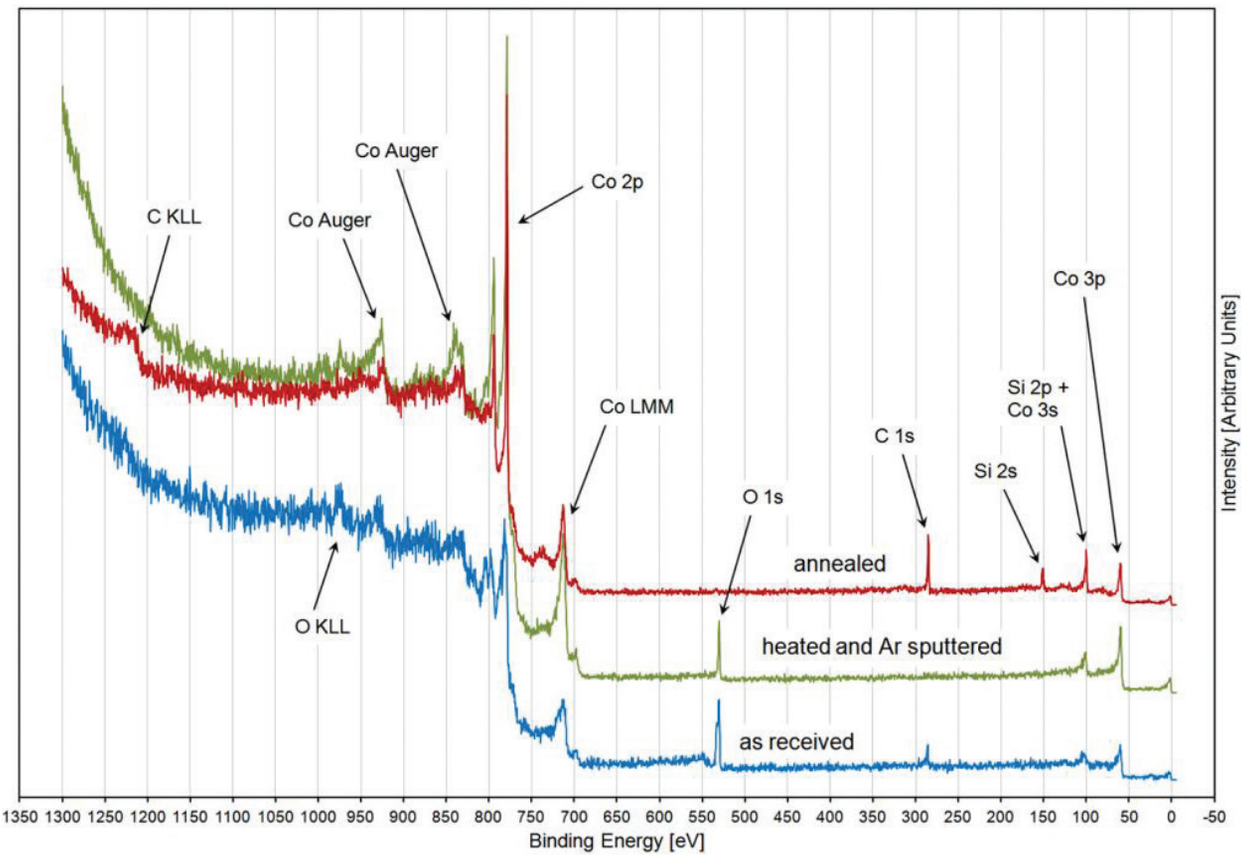

Figure 10. Survey spectra in comparison. Main found peaks are denoted. (Reprinted with permission from Thin Solid Films No. 3995281012757.).

http://dx.doi.org/10.5772/67465

Atomic concentration [%]	Si	C	O	Co
As received	0	24	40	36
Heated and Ar sputtered	0	0	23	77
Annealed	21	43	0	36

Reprinted with permission from Thin Solid Films No. 3995281012757.

Table 6. Quantification results of the atomic concentration of elements from XPS analysis.

that all spectra probably shifted to higher binding energies roughly by 0.5 eV. No software spectrum correcting was produced.

Figure 11 shows Co 2p peaks fitted by components on the basis of Ref. [37]. In the as-received state, a metallic Co component at around 779 eV, a Co^{II} and Co^{III} components at around 781 eV, and satellites at slightly higher binding energies can be identified, all confirming the native Co oxide [35–37]. As it can be anticipated, the quantity of oxide-based components was decreased by the Ar sputtering. There seems to be only metallic Co detected at the annealed sample. Cobalt is represented by an asymmetric main peak and weak plasmons [37]. Identification of

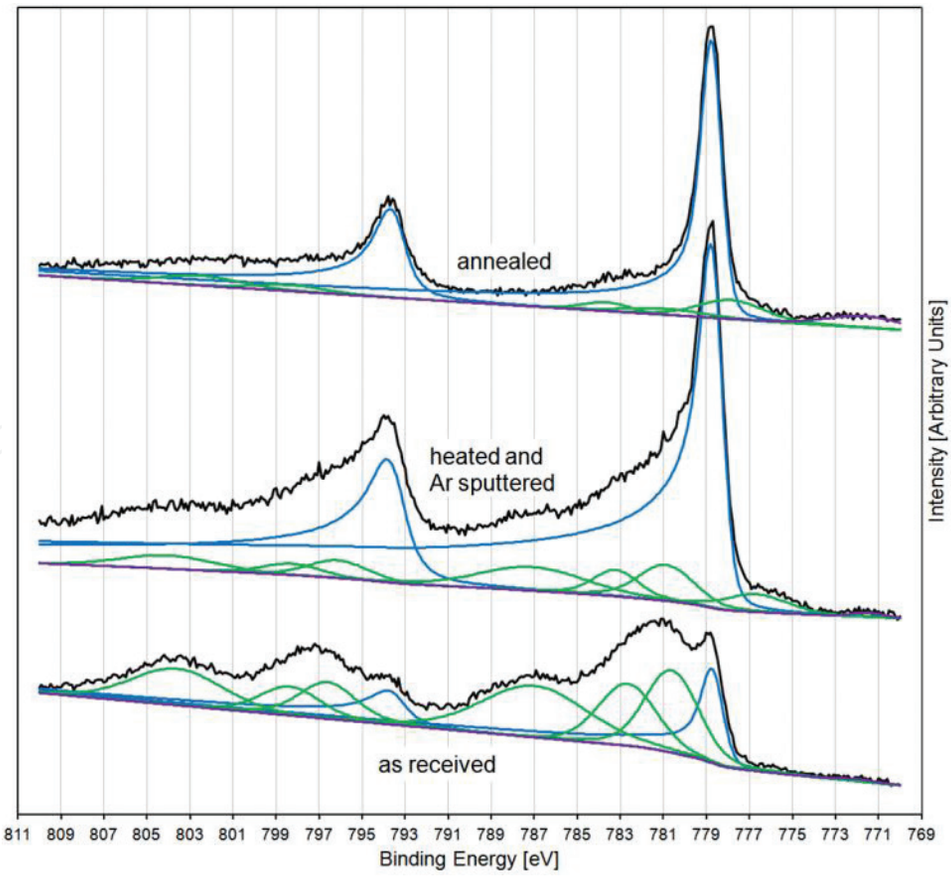

Figure 11. Co 2p in comparison. (Reprinted with permission from Thin Solid Films No. 3995281012757.).

silicide bonds by XPS is complicated [40]. But, we can suppose that Co and Si in the annealed sample create silicides. The silicides are standard reaction products in the Co/SiC system under similar reactions, and they are detected by other analytic techniques, for example, XRD [38, 39].

Information obtained from detail O 1s spectra support so far drawn suppositions. **Figure 12** shows that there are at least two chemical states of O in the as-received sample. The component at around 530.5 eV comprises O bonds in the Co oxides [35, 37]. The second component at around 532.5 eV probably belongs to disrupt oxide structure, Co hydroxides, water, and possibly impurities [35, 37]. The sputtering of the sample decreases the quantity of impurities and the oxides/hydroxides. O disappeared completely at the annealed sample.

Detail C 1s spectra, first off in comparison, are shown on **Figure 13** and with fitted components on **Figures 14** and **15**. The C 1s peak at the as-received sample can be fitted by three components; the first one positioned at 285.5 eV belongs to adventitious carbon, the second one at 287 eV, and the third one at 289.5 eV both belong to bonds between carbon and oxygen [37]. The components are standard for contamination carbon. The components can be easily removed by the argon sputtering.

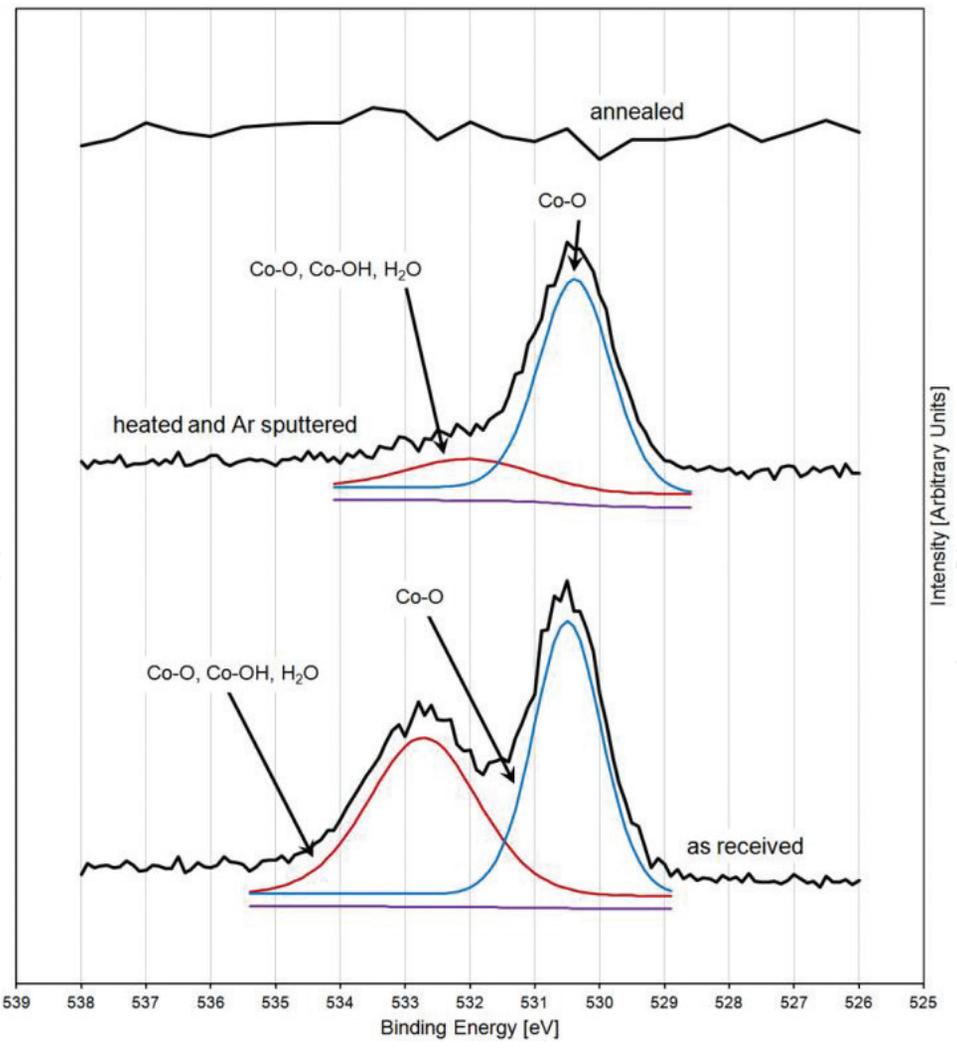

Figure 12. Fitted O 1s peaks in comparison. (Reprinted with permission from Thin Solid Films No. 3995281012757.).

http://dx.doi.org/10.5772/67465

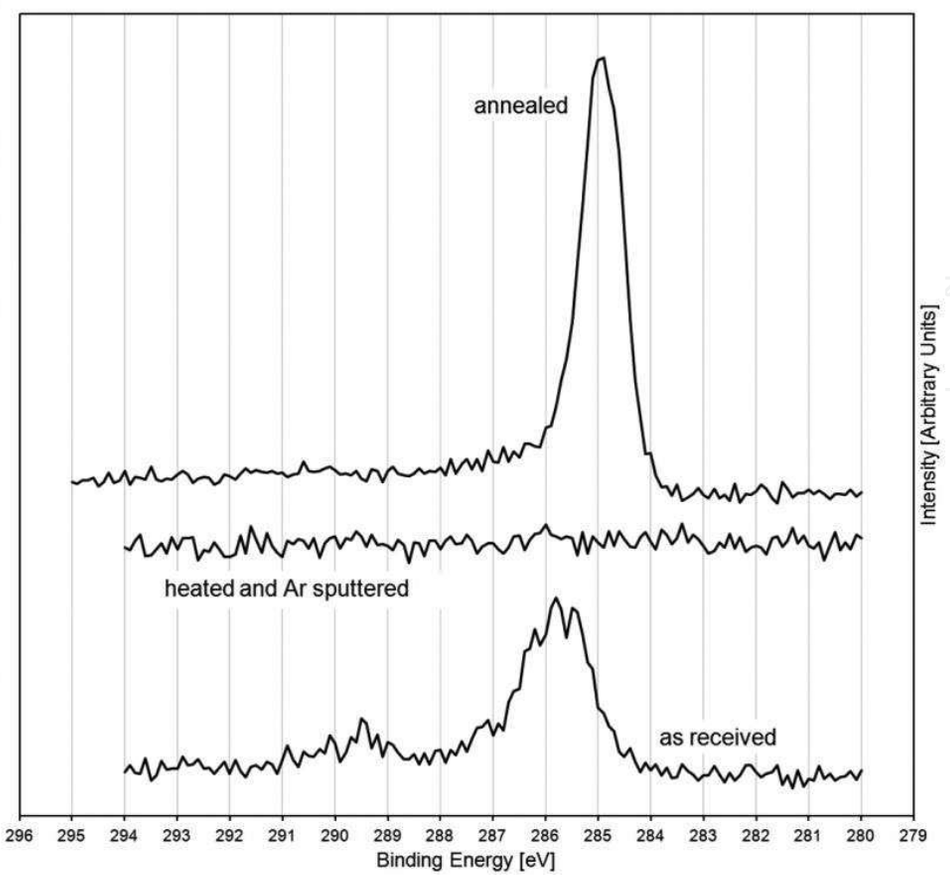

Figure 13. C 1s in comparison. (Reprinted with permission from Thin Solid Films No. 3995281012757.).

Figure 15 shows the most important carbon peak for us which was produced by the annealing. The peak is fitted with a single distinctive component positioned at 285 eV which has a relatively low FWHM (below 1 eV). C–C or C=C bonds are characteristic for the component and represent the formation of graphitic carbon phase during the annealing process [41, 42]. The peak was fitted by one symmetric component. Nevertheless, the peak shows slight asymmetry which is a mark of the metallic character of graphene [43]. The observed asymmetry of the C 1s peak in addition supports the presence of graphitic carbon.

4.5. Conclusion

The process of graphene growth was ground on an optimization of the thermal forming of the Co/SiC structure. The process was produced within a temperature range from 750 to 1080°C, and annealing time was changed in a range from 0 to 120 s. We were testing qualities of the prepared graphene films on samples' surface by the Raman spectroscopy. Nevertheless, the graphene film is also created at the metallization-SiC boundary; parameters of this so-called lower graphene are always worse than in the case of the surface graphene. This is produced by the reaction of SiC with Co leading to a large roughness of the silicon carbide surface at the interface. From the results, it is evident that the applied method produces graphene film with parameters of a bilayer one.

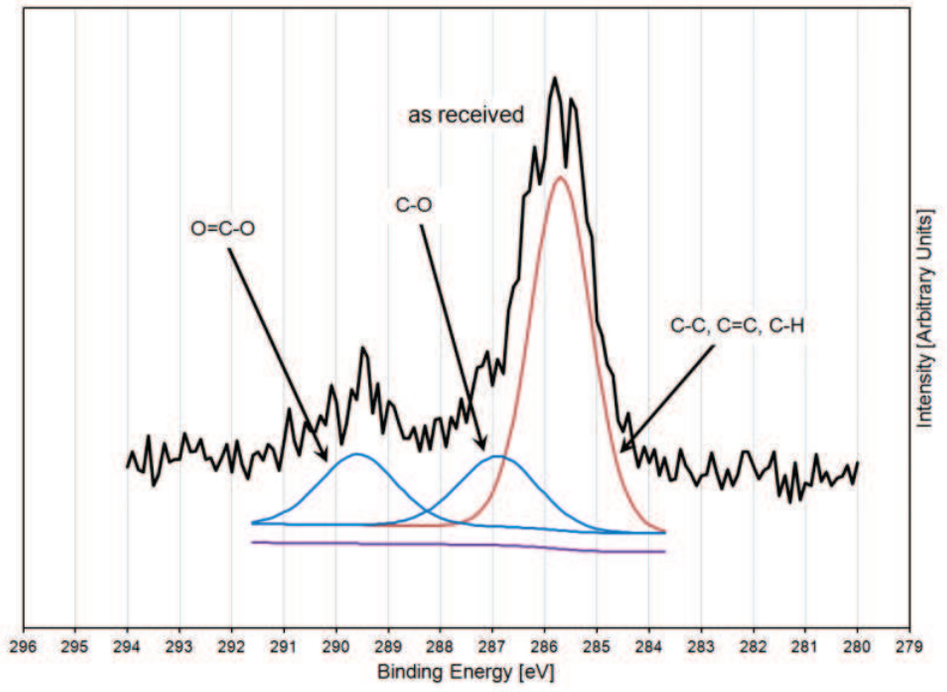

Figure 14. Fitted C 1s peak of the as-received sample. For clarity, peak components and background are vertically slightly offset. (Reprinted with permission from Thin Solid Films No. 3995281012757.).

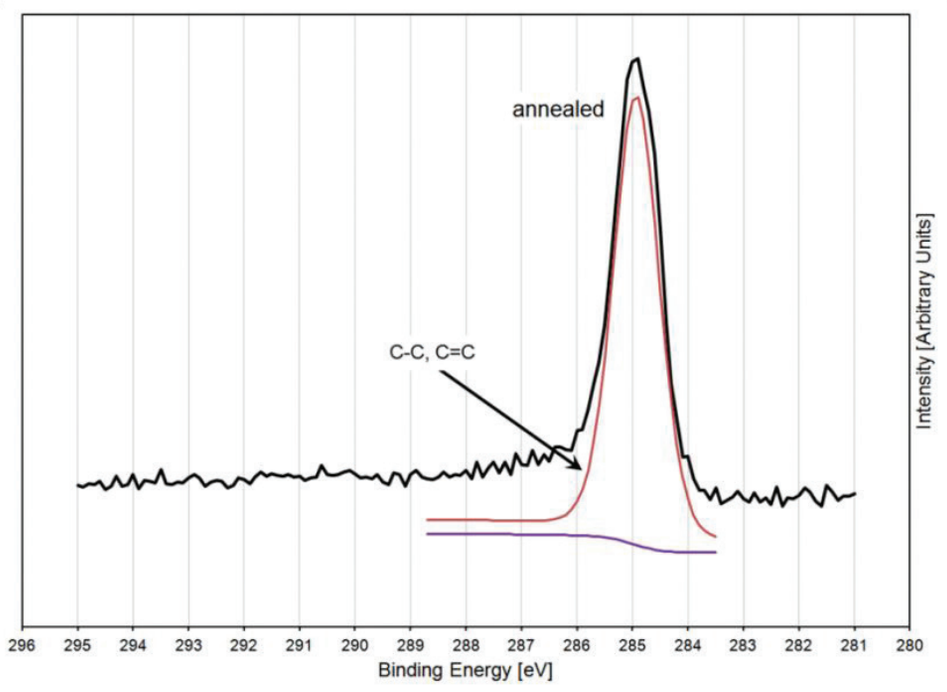

Figure 15. Fitted C 1s peak of the annealed sample. For clarity, peak components and background are vertically slightly offset. (Reprinted with permission from Thin Solid Films No. 3995281012757.).

At the Co(300 nm)/SiC structures prepared by the sputtering deposition process, the creation of two surface phases has been observed at shorter annealing period. In the case of the dark phase, the reaction between SiC and Co creates cobalt silicides and simultaneously the graphene film. Silicides and graphene are not created in the case of the light phase. By increasing the annealing time, the light-phase area shrinks, and finally it disappears. The XPS depth profiling detected a layer with increased amount of carbon atoms in the dark phase. The layer presumably represents carbon atoms that precipitate toward the surface of metallization. The precipitation is completed, and graphene is formed on the structure surface after the long experiment.

By applying the Co evaporation together with the plasma modification instead of the sputtering, the surface of the structure was homogenous and covered by the graphene film after annealing. We presuppose that the growing of the graphene film on the whole area can be attributed to a positive influence of the plasma treatment of the structure surface that was carried out just before the cobalt evaporation.

As mentioned above, it is generally postulated that parameters of the graphene films prepared by segregation depend very strictly on the CR of the structures after finishing the annealing process. Our results are different from this statement. The number of carbon monolayer in graphene has been practically independent on the CR; however, the graphene defectivity (the I_D/I_G ratio) is rapidly increasing. The possible explanation of the phenomena can be seen in the fact that the surface carbon layer (the graphene film) is formed not only by the segregation process after finishing the annealing as originally asserted but also during the annealing period. We assume that the CR modifies morphology and crystallic structure of the silicide layer and thus it increases the concentration of defects in the graphene film [44].

For the measurement of the electrical parameters, we apply the graphene film transferred onto the SiO_2/Si structure. The transfer of graphene slightly increased the graphene defectivity. The phenomenon is caused by interruption of covalent bonds between Co and carbon atoms in graphene. Unsaturated bonds are formed within the graphene due to etching off of Co, and so the number of defects in graphene film is increased [45]. Obtained value of sheet resistance is in agreement with data published in literature [45–47]. The charge carrier mobility is very small taking into consideration the maximal published values, but the graphene films with the same number of carbon monolayers produced by the CVD method [46, 48] show the charge mobility with similar or only slightly higher value. It is probably caused by the presence of significant number of defects which are absent at the best graphene structures prepared by mechanical exfoliation [4]. Grain size and cracks in the metal play a great role at the graphene transfer from polycrystalline metal substrates [46, 49]. Due to positive sign of the Hall constant, our graphene films show hole conductivity which is attributed to residues of PMMA used for the graphene transport [50].

XPS analysis of the Co/SiC structure together with its annealing and cleaning was performed in situ in the Ultra High Vacuum (UHV) apparatus. Contrary to our standard preparation process [31], special cleaning of the tested structure was performed by degassing and by Ar ions bombardment. The process significantly reduced the surface contamination. The UHV in situ structure cleaning and subsequent analysis provided clean and very well-defined

experimental conditions. In **Figure 15**, it is obvious that the Co/SiC reaction formed the graphene film on the surface of the structure as intended.

5. Application of other metals

The mentioned method is suitable for many other materials, not only for Ni and Co. Selected metals have to react with silicon carbide by the way silicides and carbon rich products are formed at the metal-SiC interface. The accumulation of graphite at the top of the metal is produced during the cooling period of the growth process. The stability or reactivity of SiC versus the number of metals was studied on the basis of phase diagrams [51]. Pd, Ge [33, 52], and Fe [53] were tested for graphene growth. In majority cases FLG was prepared.

6. Influence of additive materials

The above-described process of graphene growth is influenced by solubility of carbon within the used metal. In practice, nickel and cobalt are most frequently used; solubility of carbon in these metals is relatively high, and consequently carbon diffusion is easy. By modifying the carbon solubility in metal, it is possible to influence the quantity of carbon, which gets into the volume of metallization during the reaction of the metal with SiC, and in this way, the parameters of formed graphene are possible to influence.

Preparation of graphene was carried out on the Ni/SiC and Co/SiC structures, where the following materials were added into the metallization: germanium, copper, and gold [54]. Solubility of carbon in these materials is very low compared to Ni and Co. The main goal of the work was then to study the influence of admixtures onto parameters of prepared graphene films. Adding the admixture materials to nickel did not improve the prepared graphene films very much. Certain improvement was observed for the structures with copper, where the presence of copper in the metallization manifested itself by lowering the defect quantity of graphene. Another situation is for the metallization with cobalt. Germanium and gold did not improve the graphene parameters; however, copper proved its significant meaning. BLG (bilayer graphene) with very low defect quantity was detected on the Co structure with molar content of Cu 20% (annealing at 1000°C for 10 s).

7. Conclusion

The text of this chapter was taken from the publication of the author and his other colleagues [25, 26, 31–33, 54]. The chapter is focused on graphene preparation by silicidation of the metal/SiC structure, where nickel and cobalt were studied in the form of the metal. Graphene is formed due to SiC decomposition by annealing of the said structure at the temperature of 800–1000°C. SiC reacts with the metal to form silicides and free carbon, which

diffuses into the layer of the metal and its silicides. While cooling down the structure, carbon gets segregated onto the surface of the metallization in the form of graphene. Graphene gets formed also at the metal/SiC boundary; this lower graphene has poorer features. When using SI-SiC, it can however be used, for example, for construction of graphene transistors directly, without the need to transfer it onto a dielectric substrate.

Generally, we can say that graphene prepared from the structure containing cobalt reaches better parameters than for the structure with nickel. For the best result, preparation of bilayer graphene with low failure rate can be considered. Raman spectroscopy was chosen for the basic diagnostic method, for it is an easily accessible, nondestructive, and fast analysis.

Within the text, optimizing of graphene preparation by annealing is gradually discussed, including the questions related to the influence of cooling rate onto graphene parameters. Contrary to the results published in literature, it was found that the influence of cooling rate is negative. Further, we followed the question of the thickness of the prepared graphene using the XPS analysis. This analysis was also used for verification of graphene present on the used substrates. Surface of graphene films was studied using AFM. Transfer of graphene was carried out by means of PMMA onto the SiO_2/Si substrates. Basic electrical parameters were measured at graphene on dielectric substrates. In the closing part of the chapter, the influence of additional materials, which decrease carbon solubility in the metallization and which thus influence features of the prepared graphene film, was discussed. It was proven that the most suitable material is copper.

Graphene preparation by synthesis from the metal/SiC structure is a promising and simple method, which does not require high temperatures, complicated technological apparatuses, or handling with dangerous gasses. Therefore, the concerned method is of good prospects at graphene preparation for a number of applications. The mentioned method is very perspective for future microelectronics, because it can be used for direct growth of graphene films on semiconductor substrates (especially SiC).

Acknowledgements

The work was pursued under a financial support from the Czech Science Foundation, Project No. 17-00607S.

Author details

Petr Machac

Address all correspondence to: petr.machac@vscht.cz

Department of Solid State Engineering, University of Chemistry and Technology, Prague, Czech Republic

References

[1] W. Choi, I. Lahiri, R. Seerlabozina, Y.S. Kang, 2010 Synthesis of graphene and its applications: a review. Critical Reviews in Solid State and Materials Sciences 35 (1-2010) 52–71.

[2] M.J. Allen, V.C. Tung, R.B. Kaner, 2010 Honeycomb carbon: a review of graphene. Chemical Reviews 110 (1-2010) 132–145.

[3] T. Seyller, K.V. Emtsev, K. Gao, F. Speck, L. Ley, A. Tadich, L. Broekman, J.D. Riley, R.C.G. Leckey, O. Rader, A. Varykhalov, A.M. Shikin, 2006 Structural and electronic properties of graphite layers grown on SiC(0001). Surface Science 600 (18-2006) 3906–3911.

[4] K.S. Novoselov, A.K. Geim, S.V. Morozov, D. Jiang, Y. Zhang, S.V. Dubonos, I.V. Grigorieva, A.A. Firsov, 2004 Electric field effect in atomically thin carbon films. Science 306 (5696-2004) 666–669.

[5] K.S. Novoselov, D. Jiang, F. Schedin, T.J. Booth, V.V. Khotkevich, S.V. Morozov, A.K. Geim, 2005 Two-dimensional atomic crystals. Proceedings of the National Academy of Sciences of the United States of America (PNAS) 102 (30-2005) 10451–10453.

[6] H. Shioyama, 2001 Cleavage of graphite to graphene. Journal of Materials Science Letters 20 (6-2001) 499–500.

[7] A.N. Obraztsov, E.A. Obraztsova, A.V. Tyurnina, A.A. Zolotukhin, 2007 Chemical vapor deposition of thin graphite films of nanometer thickness. Carbon 45 (10-2007) 2017–2021.

[8] L.G. De Arco, Y. Zhang, A. Kumar, and C. Zhou, 2009 Synthesis, transfer, and devices of single- and few-layer graphene by chemical vapor deposition. IEEE Transactions on Nanotechnology 8 (2-2009) 135–138.

[9] Z.Y. Juang, C.Y. Wu, A.Y. Lu, C.Y. Su, K.C. Leou, F.R. Chen, C.H. Tsai, 2010 Graphene synthesis by chemical vapor deposition and transfer by a roll-to-roll process. Carbon 48 (11-2010) 3169–3174.

[10] W.A. de Heer, C. Berger, X. Wu, P.N. First, E.H. Conrad, X. Li, T. Li, M. Sprinkle, J. Hass, M.L. Sadowski, M. Potemski, G. Martinez, 2007 Epitaxial graphene. Solid State Communications 143 (1-2-2007) 92.

[11] S. Tanaka, K. Morita, H. Hibino, 2010 Anisotropic layer-by-layer growth of graphene on vicinal SiC(0001) surfaces. Physical Review B 81 (4-2010) 041406(R).

[12] M.L. Bolen, S.E. Harrison, L.B. Biedermann, M.A. Capano, 2009 Graphene formation mechanisms on 4*H*-SiC(0001). Physical Review B 80 (11-2009) 115433.

[13] K.V. Emtsev, A. Bostwick, K. Horn, J. Jobst, G.L. Kellogg, L. Ley, J.L. McChesney, T. Ohta, S.A. Reshanov, J. Röhrl, E. Rotenberg, A.K. Schmid, D. Waldmann, H.B. Weber, T. Seyller, 2009 Towards wafer-size graphene layers by atmospheric pressure graphitization of silicon carbide. Nature Materials 9 (3-2009) 203–207.

[14] T. Ohta, N.C. Bartelt, K. Thürmer, G.L. Kellogg, 2010 Role of carbon surface diffusion on the growth of epitaxial graphene on SiC. Physical Review B 81 (12-2010) 121411(R).

[15] M.E. Ayhan, G. Kalita, R. Papon, R. Hirano and M. Tanemura, 2014 Synthesis of transfer-free graphene by solid phase reaction process in presence of a carbon diffusion barrier. Materials Letters 129, 76–79.

[16] Q. Zhuo, Q. Wang, Y. Zhang, D. Zhang, Q. Li, C. Gao, Y. Sun, L. Ding, Q. Sun, S. Wang, J. Zhong, X. Sun, S. Lee, 2015 Transfer-free synthesis of doped and patterned graphene films. ACS Nano 9 (1-2015) 594–601.

[17] A. Delamoreanu, C. Rabot, C. Vallee and A. Zenasni, 2014 Wafer scale catalytic growth of graphene on nickel by solid carbon source. Carbon 66, 48–56.

[18] Z.Y. Juang, C.Y. Wu, C.W. Lo, W.Y. Chen, C.F. Juany, J.C. Hwang, F.R. Chen, K.C. Leou, C.H. Tsai, 2009 Synthesis of graphene on silicon carbide substrates at low temperature. Carbon 47 (11-2009) 2026–2031.

[19] A.A. Woodworth, C.D. Stinespring, 2010 Surface chemistry of Ni induced graphite formation on the 6H–SiC (0001) surface and its implications for graphene synthesis. Carbon 48 (7-2010) 1999–2003.

[20] T. Yoneda, M. Shibuya, K. Mitsuhara, A. Visikovskiy, Y. Hoshino, Y. Kido, 2010 Graphene on SiC(0001) and SiC(000(1)over-bar) surfaces grown via Ni-silicidation reactions. Surface Science 604 (17-18-2010) 1509–1515.

[21] K. Vassilevski, I.P. Nikitina, A.B. Horsfall, N.G. Wright, C.M. Johnson, 2010 Epitaxial graphene elaborated on 3C-SiC(111)/Si epilayers. Materials Science Forum 645–648, 589–592

[22] J. Hofrichter, B.N. Szafranek, M. Otto, T.J. Echtermeyer, M. Baus, A. Majeru, V. Geringer, M. Ramsteiner, H. Kurz, 2010 Synthesis of graphene on silicon dioxide by a solid carbon source. Nano Letters 10 (1-2010) 36–42.

[23] C. Li, D. Li, J. Yang, X. Zeng, W. Yuan, 2011 Preparation of single and few layer graphene sheets using Co depositing on SiC substrate. Journal of Nanomaterials 2011 (2011) 319624.

[24] B.V. Cunning, M. Ahmed, N. Mishra, A.R. Kermany, B. Wood, F. Iacopi, 2014 Graphitized silicon carbide microbeams: wafer-level, self-aligned graphene on silicon wafers. Nanotechnology 25 (32-2014) 325301.

[25] P. Machac, T. Fidler, S. Cichon, L. Miskova, 2012 Synthesis of graphene on SiC substrate via Ni-silicidation reactions. Thin Solid Films 520 (2012) 5215–5218.

[26] P. Machac, T. Hrebicek, 2016 Synthesis of graphene on Ni/SiC structure. Journal of Electrical Engineering 67 (2-2016) 147–149.

[27] M.A. Pimenta, G. Dresselhaus, M.S. Dresselhaus, L.G. Cancado, A. Jorio, R. Saito, 2007 Studying disorder in graphite-based systems by Raman spectroscopy. Physical Chemistry Chemical Physics 9 (11-2007) 1276–1291.

[28] Y. Hao, Y. Wang, L. Wang, Z. Ni, Z. Wang, R. Wang, C.K. Koo, Z. Shen, J.T.L. Thong, 2010 Probing layer number and stacking order of few-layer graphene by Raman spectroscopy. Small 6 (2-2010) 195–200.

[29] S. Tanuma, C.J. Powell, D.R. Penn, 1991 Calculations of electron inelastic mean free paths II. Data for 27 elements over the 50-2000 eV range. Surface and Interface Analysis 17 (13-1991), 911–926.

[30] Y. Wu, W. Ren, L. Gao, B. Liu, C. Jiang, H. Cheng, 2009 Synthesis of high-quality graphene with a pre-determined number of layers. Carbon 47 (2-2009) 493–499.

[31] P. Machac, T. Fidler, S. Cichon, V. Jurka, 2013 Synthesis of graphene on Co/SiC structure. Journal of Materials Science: Materials in Electronics 24 (10-2013) 3793–3799.

[32] P. Machac, S. Cichon, L. Miskova, M. Vondracek, 2014 Graphene preparation by annealing of Co/SiC structure. Applied Surface Science 320 (2014) 544–551.

[33] P. Machac, T. Fidler, S. Cichon, 2013 Graphene preparation by annealing of metal/SiC structure. Proceedings EDS'13 IMAPS CS International Conference Brno, Czech Republic, June 26–27, 2013, 11–14.

[34] A. Umair, H. Raza, 2012 Controlled synthesis of bi-layer graphene on nickel. Nanoscale Research Letters 7 (1-2012) 437–440.

[35] A. Galtayries, J. Grimblot, 1999 Formation and electronic properties of oxide and sulphide films of Co, Ni and Mo studied by XPS. Journal of Electron Spectroscopy and Related Phenomena 98–99 (1-1999) 267–275.

[36] J.G. Dillard, H. Glasbrenner, G. Pfennig, H. Klewe-Nebenius, H.J. Ache, 1990 Surface-analysis studies of Zr-Co alloy and Zr-Co alloy-films. Journal of the Less-Common Metals 166 (2-1990) 233–239.

[37] M.C. Biesinger, B.P. Payne, A.P. Grosvenor, L.W.M. Lau, A.R. Gerson, R.St.C. Smart, 2011 Resolving surface chemical states in XPS analysis of first row transition metals, oxides and hydroxides: Cr, Mn, Fe, Co and Ni. Applied Surface Science 257 (7-2011) 2717–2730.

[38] S.W. Park, Y.I. Kim, J.S. Kwak, H.K. Baik, 1997 Investigation of Co/SiC interface reaction. Journal of Electronic Materials 26 (3-1997) 172–177.

[39] T. Fujimura, S.I. Tanaka, 1999 In-situ high temperature X-ray diffraction study of Co/SiC interface reactions. Journal of Materials Science 34 (23-1999) 5743–5747.

[40] P.L. Tam, Y. Cao, L. Nyborg, 2012 XRD and XPS characterisation of transition metal silicide thin films. Surface Science 606 (3-4-2012) 329–336.

[41] U. Starke, C. Riedl, 2009 Epitaxial graphene on SiC(0001) and SiC(000ī): from surface reconstructions to carbon electronics. J. Phys: Condensed Matter. 21 (13-2009) 134016.

[42] E. Rollings, G.H. Gweon, S.Y. Zhou, B.S. Mun, J.L. McChesney, B.S. Hussain, A.V. Fedorov, P.N. First, W.A. de Heer, A. Lanzara, 2006 Synthesis and characterization of atomically thin graphite films on a silicon carbide substrate. Journal of Physics and Chemistry of Solids 67 (9-10-2006) 2172–2177.

[43] M. Ostler, F. Speck, M. Gick, T. Seyller, 2010 Automated preparation of high-quality epitaxial graphene on 6H-SiC(0001). Physica Status Solidi B – Basic Solid State Physics 247 (11-12-2010) 2924–2926.

[44] H. Ago, Y. Ito, N. Mizuta, K. Yoshida, B. Hu, C.M. Orofeo, M. Tsuji, K. Ikeda, S. Mizuno, 2010 Epitaxial chemical vapor deposition growth of single-layer graphene over cobalt film crystallized on sapphire. ACS Nano 4 (11-2010) 7407–7414.

[45] N. Liu, L. Fu, B. Dai, K. Yan, X. Liu, R. Zhao, Y. Zhang, Z. Liu, 2011 Universal segregation growth approach to wafer-size graphene from non-noble metals. Nano Letters 11 (1-2011) 297–303.

[46] A. Reina, X. Jia, J. Ho, D. Nezich, H. Son, V. Bulovic, M.S. Dresselhaus, J. Kong, 2009 Large area, few-layer graphene films on arbitrary substrates by chemical vapor deposition. Nano Letters 9 (1-2009) 30–35.

[47] A. Reina, S. Thiele, X. Jia, S. Bhaviripudi, M.S. Dressehaus, J.A. Schaefer, J. Kong, 2009 Growth of large-area single- and Bi-layer graphene by controlled carbon precipitation on polycrystalline Ni surfaces. Nano Research 2 (6-2009) 509–516.

[48] X. Li, W. Cai, J. An, S. Kim, J. Nah, D. Yang, R. Piner, A. Velamakanni, I. Jung, E. Tutuc, S.K. Banerjee, L. Colombo, R.S. Ruoff, 2009 Large-area synthesis of high-quality and uniform graphene films on copper foils. Science 324 (5932-2009) 1312–1314.

[49] S. Thiele, A. Reina, P. Healey, J. Kedziersky, P. Wyatt, P.L. Hsu, C. Keast, J. Schaefer, J. Kong, 2010 Engineering polycrystalline Ni films to improve thickness uniformity of the chemical-vapor-deposition-grown graphene films. Nanotechnology 21 (1-2010) 015601.

[50] J. Kang, D. Shin, S. Bae, B.H. Hong, 2012 Graphene transfer: key for applications. Nanoscale 4 (1-2012) 5527–5537.

[51] J.C. Schuster, 1993 Silicon carbide and transition metals: a critical evaluation of existing phase diagram data supplemented by new experimental results. International Journal of Refractory Metals and Hard Materials 12 (4-1993-1994) 173–177.

[52] H. Hiura, M.V. Lee, A.V. Tyurnina, K. Tsukagoshi, 2012 Liquid phase growth of graphene on silicon carbide. Carbon 50 (14-2012) 5076–5084.

[53] S.P. Cooil, F. Song, G.T. Williams, O.R. Roberts, D.P. Langstaff, B. Jorgensen, K. Hoydalsvik, D.W. Breiby, E. Wahlstrőm, D.A. Evans, J.W. Wells, 2012 Iron-mediated growth of epitaxial graphene on SiC and diamond. Carbon 50 (14-2012) 5099–5105.

[54] T. Hrebicek: Graphene preparation by silicidation of the structure metal/SiC. Diploma Thesis, University of Chemistry and Technology, Prague, Czech Republic, 2016.

IntechOpen